

Electrical Conductances of Tetrabutylammonium and Decamethylferrocenium Hexafluorophosphate in Organic Solvents

Darío L. Goldfarb,^{1,3} María Paula Longinotti,¹ and Horacio R. Corti^{1,2*}

Received June 1, 2000; revised December 15, 2000

The electrical conductances of tetrabutylammonium hexafluorophosphate in acetone and of decamethylferrocenium hexafluorophosphate in acetone, acetonitrile, 1,2-dichloroethane, and dichloromethane have been measured at 25°C. The Walden product of the Bu_4N^+ cation and the PF_6^- anion in acetone and other solvents is discussed in relation to the dielectric friction. The electric conductance at infinite dilution and the association constant of decamethylferrocenium hexafluorophosphate were determined in the four solvents investigated. The association constant of this electrolyte increases with decreasing reduced temperature, as expected in the framework of the association theory, within the primitive model of electrolytes.

KEY WORDS: Conductance; association constant; organic solvents; dielectric friction; decamethylferrocenium hexafluorophosphate; acetone; acetonitrile; 1,2-dichloroethane; dichloromethane; tetrabutylammonium hexafluorophosphate.

1. INTRODUCTION

The use of microelectrodes to determine diffusion coefficients in highly resistive media by voltammetric techniques, even in the absence of supporting electrolyte, has opened an interesting field to investigate the effect of ionic association on transport properties.^(1,2) High-resistance systems of interest include organic solvents of low dielectric constant⁽³⁾ and supercritical solutions having low dielectric constant and density.⁽⁴⁾

¹Comisión Nacional de Energía Atómica, Unidad de Actividad Química Av. Gral. Paz 1499 (1650) San Martín, Buenos Aires, Argentina.

²Escuela de Ciencia y Tecnología, Universidad Nacional de General San Martín, Calle 78, No. 3901, (1653) Villa Ballester, Buenos Aires, Argentina. Email hrcorti@cnea.gov.ar

³Present address: Department of Chemical Engineering, University of Wisconsin, Madison Wisconsin.

In these systems, the solubility of simple salts is very low, while more soluble salts containing bulky ions are strongly associated. Recently,⁽⁵⁾ we explored the use of tetrabutylammonium hexafluorophosphate (Bu_4NPF_6) and decamethylferrocenium hexafluorophosphate [$\text{Fe}(\text{Cp}^*)_2\text{PF}_6$, with $\text{Cp}^* = \eta_5\text{-C}_5\text{Me}_5$] as support and electroactive electrolytes, respectively, in supercritical solvents. The complex behavior of transport properties in supercritical systems can not be well understood if the behavior in low-electrical permittivity solvents is not adequately analyzed.

The strategy of this work is as follow: (1) from the knowledge of the limiting ionic conductivity of the tetrabutylammonium (Bu_4N^+) cation as a function of solvent properties (viscosity and permittivity) and the limiting ionic conductivity of the Bu_4NPF_6 in low-dielectric constant solvents, the behavior of the limiting conductivity of the hexafluorophosphate (PF_6^-) anion over a wide range of permittivities will be analyzed. (2) The measurements of the limiting conductivity of $\text{Fe}(\text{Cp}^*)_2\text{PF}_6$ in different solvents will enable the limiting conductivity of the decamethylferrocenium [$\text{Fe}(\text{Cp}^*)_2^+$] cation to be estimated.

Following the procedures indicated in Table I, the ionic conductivity of the Bu_4N^+ ion has been determined in a large number of solvents,⁽⁶⁻²⁰⁾ covering a wide range of dielectric constants. Values arising from direct measurements of ionic conductivity (transport number measurements) were separated from those which incorporated an approximation for the relation between the anionic and cationic conductance. It can be observed that, except for a few solvents (water, sulfolane, and ethylene glycol), the Walden product (limiting ionic conductivity \times viscosity product) lie in the range $21.5 \pm 1.5 \text{ S-cm}^2\text{-mol}^{-1}\text{-mPa-s}$.

The electrical conductivity of hexafluorophosphate salts has been studied in water⁽²¹⁾ and few organic solvents, such as propylene carbonate,^(22,23) dimethyl sulfoxide,⁽²⁴⁾ sulfolane,⁽²⁵⁾ acetonitrile⁽⁶⁾ and dichloromethane.⁽²⁶⁾ It should be noted that the reported limiting conductivity of Bu_4NPF_6 in dichloromethane has an uncertainty larger than 1%. The results summarized in Table II show that the Walden product for the PF_6^- anion exhibits a clear dependence on the dielectric constant, which is related to the contribution of dielectric friction in the case of this small ion. Since there is shortage of accuracy data for the PF_6^- anion in the low dielectric constant range ($\epsilon < 35$), the molar conductivity of Bu_4NPF_6 in acetone ($\epsilon = 20.7$) was measured in this work in order to extend the permittivity range.

The lack of information on the $\text{Fe}(\text{Cp}^*)_2^+$ ion prompted us to measure the electrical conductivity of its hexafluorophosphate salt in low-permittivity organic solvents with dielectric constants ranging from 36.7 (acetonitrile) to 8.93 (dichloromethane) where high ion association is expected.

Limiting molar conductivity Λ^0 and association constants K_A for ion-pair formation can be obtained from conductivity measurements of electrolyte solutions.⁽²⁷⁾ This information will be used to analyze ion association and type of friction taking part in the transport process of these species in different solvents.

Table I. Walden Products and Hubbard–Onsager Radii for the Bu_4N^+ ion^a

Solvent	$T(^{\circ}\text{C})$	ε	$\eta(\text{mPa}\cdot\text{s})$	$\lambda^0\eta$	Ref. ^b	R_{HO} (nm)
Formamide	25	111.0	3.30	22.5 21.5 ₇	6 (A) 7 (A)	0.146
2-Cyanopyridine	30	93.8	1.82	22.0	8 (B)	
Ethylene carbonate	40	90.4	1.93	22.5	8 (B)	
Dimethylmetanosulfonamide	50	80.31	3.150	23.0 ₆	8 (B)	
3-Methyl-2-oxazolidone	25	77.5	2.45	22.3	8 (B)	
Water	25	78.54	0.8937	17.40	9 (A)	0.150
Propylene carbonate	25	64.92	2.513	22.5 ₆ 22.6 ₂	10 (A) 11 (A)	0.184
Dimethyl sulfoxide	25	46.6	1.963	23.2 21.4 ₆	6 (A) 7 (A)	0.175
Sulfolane	30	43.3	10.286	28.4	6 (A)	
Ethylene glycol	25	40.29	16.61	25.1	6 (A)	0.165
Dimethylacetamide	25	37.8	0.919	21.0 ₅	7 (A)	
Dimethylformamide	25	37.6	0.796	20.2 21.1 ₆	6 (A) 7 (A)	0.196
Nitromethane	25	36.7	0.612	20.9 21.3 ₆	6 (A) 7 (A)	0.166
Acetonitrile	25	35.9	0.344	21.1 21.2 ₂	6 (A) 7 (A)	0.183
2-Methylpyridine <i>N</i> -oxide	25	35.65	3.371	23.0	12 (B)	
Nitrobenzene	25	34.3	1.849	21.3 ₅	13 (A)	0.229
Methanol	25	32.6	0.545	21.3 21.3 ₃	6 (A) 7 (A)	0.332
Hexamethylphosphotriamide	25	29.6	3.23	20.6 ₇	14 (A)	0.241
Ethanol	25	24.3	1.084	21.4 21.3 ₁	6 (A) 7 (A)	0.399
<i>i</i> -Butyronitrile	25	23.81	0.485	20.5 ₇	15 (A)	
Tetramethylurea	25	23.4	1.401	21.6 ₇	7 (A)	
Acetone	25	20.7	0.3116	20.9 ₁	16 (A)	0.210
1-Propanol	25	20.5	1.947	21.4 ₂	7 (A)	0.428
2-Propanol	25	19.4	2.078	21.0 ₇	17 (A)	
2-Butanone	25	18.04	0.3676	19.4 ₄	18 (C)	
1-Butanol	25	17.45	2.589	20.3 ₀	7 (A)	0.456
2-Metoxiethanol	25	16.9	1.601	22.6 ₁	19 (D)	
Pyridine	25	12.0	0.8824	20.0 ₀	19 (D)	
Methylformate	25	8.90	0.328	21.0	20 (E)	

^aUnits: Walden Product $\text{S}\cdot\text{cm}^2\cdot\text{mol}^{-1}\cdot\text{mPa}\cdot\text{s}$.

^b(A) Calculated from experimental data; (B) assuming $\lambda^0(i\text{-Pe}_3\text{BuN}^+) = \lambda^0(\text{BPh}_4^-)$; (C) assuming $\lambda^0(i\text{-Am}_3\text{BuN}^+) = \lambda^0(\text{BPh}_4^-)$; (D) assuming $\lambda^0(\text{Bu}_4\text{N}^+) = \lambda^0(\text{BBu}_4^-)$; (E) assuming $\lambda^0\eta = 0.8204/[5.00 - (0.0103\varepsilon + 0.85)]$ (Ref. 16).

Table II. Walden Product for the PF_6^- Ion

Solvent	$T(^{\circ}\text{C})$	ϵ	$\eta(\text{mPa}\cdot\text{s})$	$\lambda^0\eta$	Ref. (Method) ^a
Water	25	78.54	0.8937	53.0	21 (A)
	50	70.10	0.5496	50.5	21 (A)
Propylene carbonate	25	64.92	2.513	44.2 ₃	22 (A)
				41.9 ₇	23 (A)
Dimethyl sulfoxide	25	46.6	1.963	45.4 ₄	24 (F)
Sulfolane	30	43.3	10.286	61.2	25 (A)
Acetonitrile	25	35.9	0.344	35.6	6 (A)
Acetone	25	20.7	0.3116	36.0 ₂	This work
Dichloromethane	25	8.93	0.413	29	26 (A)

^a(A) calculated from experimental data; (F) assuming $\lambda^0(i\text{-Am}_4\text{N}^+) = \lambda^0(i\text{-Am}_4\text{B}^-)$ and using the transport number of KI.

2. EXPERIMENTAL

Dichloromethane (Baker, HPLC grade) and 1,2-dichloroethane (Aldrich, >99%) were distilled previous to use. Acetonitrile (Baker, HPLC grade) and acetone (Aldrich, >99.9%) were used without further purification.

Tetrabutylammonium hexafluorophosphate (Fluka, electrochemical grade) was used as-received. Decamethylferrocenium hexafluorophosphate was synthesized and purified following a literature procedure.⁽²⁸⁾ All solids were stored in vacuum desiccators.

Two conductivity cells were employed. CELL1 was a conventional glass cell with mixing bulb, already employed to determine the conductivity of aqueous electrolytes with a high degree of precision.⁽²⁹⁾ The cell constant, $k_{\text{cell}} = 13.511 \pm 0.004 \text{ m}^{-1}$ at 25°C, was measured using standard KCl solutions of known specific conductivity.⁽³⁰⁾

Initially, the solvent was added under a N_2 atmosphere and the cell was thermostated in a kerosene-oil bath (125 dm³) at 25°C \pm 0.002°C. The temperature was controlled with a contact thermometer. The thermal bath experienced very low over/undershooting on the temperature control because of its high overall heat capacity. After reaching thermal equilibrium, the solvent resistance was measured and a weighted amount of solid added to the cell in a small glass thimble. The solution was homogenized by stirring and again placed in the thermostatic bath. The solution resistance was recorded at several frequencies between 0.5 and 10 kHz and new amounts of solid were added to the cell.

Because of the high ionic association of the salt studied in this work in solvents of low permittivity, CELL1 was not adequate for accurate measurements in highly resistive media. We used a novel cell design (CELL2) fashioned after that described by Younglove and Straty,⁽³¹⁾ which was originally constructed to obtain dielectric constant data of pure water from capacitive measurements. It consisted

of cylindrical electropolished SS316 electrodes in a concentric geometry. The external SS316 body of the cell was grounded and electrically isolated from the electrode assembly. A magnetic bar was used for stirring the solutions inside the cell. A further description of this cell can be found elsewhere.⁽³²⁾

The cell constant was calculated from a capacitance measurement under vacuum using the relationship

$$C(T, p = 0) = \varepsilon_0 k_{\text{cell}} \quad (1)$$

with ε_0 the permittivity of vacuum ($8.85419 \cdot 10^{-12} \text{ F}\cdot\text{m}^{-1}$). The values of k_{cell} were $0.27473 \pm 0.00002 \text{ m}^{-1}$ at 25°C and $0.27457 \pm 0.00002 \text{ m}^{-1}$ at 50°C .

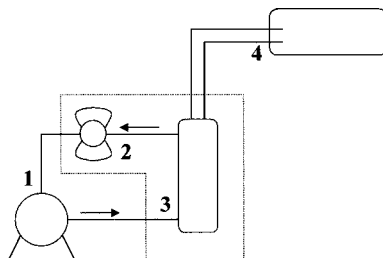
As can be noticed, CELL2 has a k_{cell} about 50 times smaller than CELL1, and it was used to measure the electrical resistance of those solutions prepared with solvents of lower dielectric constant (dichloromethane and 1,2-dichloroethane). In these solvents, extensive ion pairing was expected and very low electrical conductivities were measured because of the low concentration of free ions. For acetone and acetonitrile, CELL1 was employed, where the dissociation degree was higher and lower resistances were encountered even at low salt concentration.

CELL2 was part of a closed circuit (Fig. 1) of known volume. The total volume was calculated by pressurizing the system with nitrogen up to 50 bar. Pressure was read with a pressure transducer (Burster 0–200 bar) calibrated using a dead-weight balance (Ruska). The gas was vented in an inverted volumetric flask (2 dm^3) filled with nitrogen-saturated water. The weight difference for the water contained in the flask before and after venting the gas together with the pressure drop due to the venting process and the equation of state for nitrogen was used to calculate the overall volume.

Initially, the system is filled with a solution of known analytical concentration containing the salt to be measured and recirculated by means of an HPLC pump (Gilson 305).

Small additions of concentrated standards were made to the system through two calibrated loops connected to a 10-way injection valve (Valco) thermostated at 25°C . Since every injection involved a replacement of a known small volume of the solution contained in the closed circuit for the injection standard (a more

Fig. 1. Experimental setup for conductivity measurements using CELL2. (1) HPLC pump; (2) 10-way injection valve; (3) CELL2; (4) impedance analyzer. Broken lines indicated the thermostated parts of the setup.



concentrated solution), the resulting concentration in the closed circuit was calculated by taking into account the volume injected and extracted from the system (salt concentrations were always $<7 \times 10^{-4} \text{ mol-dm}^{-3}$, and the solution density can be approximated by that of the pure solvent). Thermostatic control was achieved with a thermostatic head (Termomix) and the water bath was controlled to $\pm 0.05^\circ\text{C}$. Temperature was measured with a calibrated platinum resistor thermometer.

For the resistance measurements, a Precision Component Analyzer (Wayne Kerr 6425) generated the AC voltage applied to the electrodes (100 mV) at different frequencies and registered the resistive component R of the complex impedance. Electric polarization was eliminated from conductivity measurements by extrapolating resistance values to infinite frequency.

3. RESULTS AND DISCUSSION

3.1. Treatment of Data

The conductance data were analyzed using a computer program described by Fuoss and Hsia,⁽³³⁾ which utilizes the Fuoss–Hsia–Fernández Prini (FHFP) equation⁽³⁴⁾

$$\Lambda = \Lambda^0 - S(\alpha c)^{1/2} + E\alpha c \ln(\alpha c) + J_1(d)\alpha c - J_2(d)(\alpha c)^{3/2} - K_A \Lambda \gamma_{\pm}^2(\alpha c) \quad (2)$$

where c is the molar concentration, α is the degree of dissociation (so that αc is the concentration of free ions), and K_A is the association constant for ion pairs. S , E , J_1 and J_2 were calculated using the equations given by Fernández Prini⁽³⁴⁾ using viscosity and dielectric constant data. The mean activity coefficients of the free ions γ_{\pm} were obtained from the Debye–Hückel limiting law:

$$\ln \gamma_{\pm} = - \frac{A(\alpha c)^{1/2}}{1 + d\kappa} \quad (3)$$

where κ is the reciprocal radius of the ionic atmosphere and the parameter d (distance of closest approach of ions) was set equal to the Bjerrum distance in accord with the procedure outlined by Justice.⁽³⁵⁾

The degree of dissociation α is related to the association constant K_A in the molarity scale through:

$$K_A = \frac{(1 - \alpha)}{\gamma_{\pm}^2 \alpha^2 c} \quad (4)$$

A nonlinear least-squares fitting of this equation to sets of (Λ, c) allowed the calculation of the two parameters Λ^0 and K_A .

For a couple of very associated systems [Bu_4NPF_6 in dichloromethane at 25°C and $\text{Fe}(\text{Cp}^*)_2\text{PF}_6$ in 1,2-dichloroethane at 50°C] measured with CELL2,

the accuracy and the amount of experimental data were not enough to achieve convergence using the above described procedure. Therefore, we employed, in this case, the method of Fuoss and Krauss (FK),⁽³⁶⁾ including the approximate Debye–Hückel and Onsager’s corrections for activity coefficients and conductance.

$$\frac{T(z)}{\Lambda} = \frac{1}{\Lambda^0} + \frac{c\gamma_{\pm}^2\Lambda}{T(z)} \frac{K_A}{(\Lambda^0)^2} \quad (5)$$

where

$$T(z) = 1 - z[1 - z(1 - \dots)^{-1/2}] - 1/2 \approx 1 - z \quad (6)$$

and

$$z = \frac{S(\Lambda c)^{1/2}}{(\Lambda^0)^{3/2}} \quad (7)$$

Λ^0 and K_A can be calculated using Eq. (5) from a plot of $T(z)/\Lambda$ vs. $c\gamma_{\pm}^2\Lambda/T(z)$, through an iterative procedure: an initial guess for Λ^0 is used to calculate $T(z)$, which enables a linear least-square regression to be made and a new value for Λ^0 to be obtained from the intercept. The calculus is repeated until convergence is reached. K_A is obtained from the slope (K_A/Λ^0).

There is no evidence of triple ion formation in these measurements as evidenced by the lack of a minimum in the plots of Λ vs. c .

3.2. Electrical Conductivity of Bu₄NPF₆ in Acetone

The measured molar conductivity of Bu₄NPF₆ in acetone at 25°C are shown in Table III. The precision of the measurements in acetone (*ca.* 0.05%) allowed the treatment of the concentration dependence of the molar conductivity by the FHFP, Eq. (2). Deviations of the experimental data from the calculated best fit ($\Lambda^{\text{exp}} - \Lambda^{\text{calc}}$) are shown in Fig. 2. The limiting conductance and ion association constant obtained from these data using the Bjerrum distance in Eq. (2) were $182.7 \pm 0.4 \text{ S-cm}^2\text{-mol}^{-1}$ and $78 \pm 4 \text{ dm}^3\text{-mol}^{-1}$, respectively.

Table III. Molar Conductivities of Bu₄NPF₆ in Acetone at 25°C

$10^3 c \text{ (mol-dm}^{-3}\text{)}$	$\Lambda \text{ (S-cm}^2\text{-mol}^{-1}\text{)}$
0.05800	176.95
0.10104	175.28
0.14090	173.52
0.20552	171.69
0.29556	169.61
0.42107	166.72
0.55951	164.21

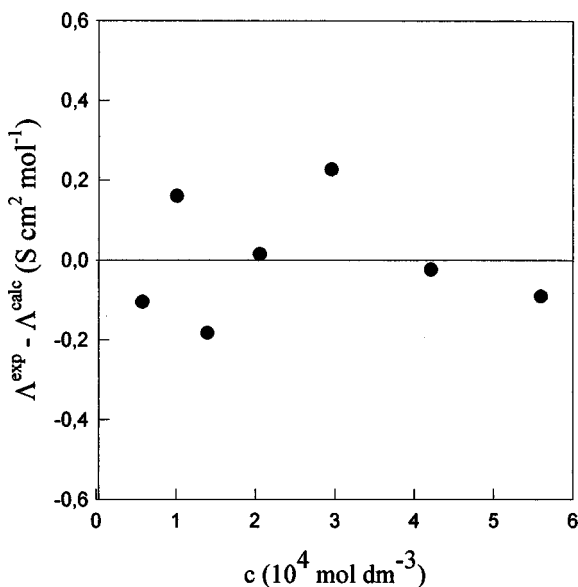


Fig. 2. Conductivity data for Bu_4NPF_6 in acetone at 25°C expressed as deviations from Eq. (8) with the parameters reported in Table IV.

Using the ionic conductivity of the Bu_4N^+ cation in acetone reported in Table I, we assigned the ionic conductivity for the PF_6^- ion shown in Table II.

3.3. Viscous and Dielectric Friction of Bu_4N^+ and PF_6^- Ions in Organic Solvents

The Bu_4N^+ ion does not show a noticeable dependence of $\lambda^0\eta$ on ϵ , indicating that the simple viscous friction model expressed by the Stokes–Einstein equation:

$$\lambda^0 = \frac{z^2 e F}{A \pi r \eta_0} \quad (8)$$

could be valid. In this model the electrical conductivity is determined by the charge ze and the hydrodynamic radius r of the ion and the viscosity η_0 of the solvent. A is a constant, which depends on the boundary conditions (four for slip and six for stick). The hydrodynamic radius of the Bu_4N^+ ion, obtained from the average Walden products of Table I ($21.2 \text{ S-cm}^2\text{-mol}^{-1}\text{-mPa-s}$) and Eq. (8), is 0.580 nm for slip and 0.387 nm for stick conditions. The crystallographic radius of the Bu_4N^+ ion is 0.494 nm ,⁽³⁷⁾ which indicates that the slipping conditions are closer to the experimental values but the Stokes–Einstein equation under slip conditions overestimates the ion mobility, if the crystallographic radius is used.

The excess of friction of an ion over the viscous regime could be ascribed to the dielectric friction. Zwanzig's⁽³⁸⁾ theory of the dielectric friction leads to the following results in terms of the Walden product:

$$\frac{z^2 e F}{\lambda^0 \eta_0} = A_V \pi r + A_D \frac{Q}{r^3} \quad (9)$$

where $A_V = 6$, $A_D = 3/8$ for stick conditions and $A_V = 4$, $A_D = 3/4$ for slip conditions. Q is a parameter defined in terms of the static dielectric constant ϵ_0 , the infinite frequency dielectric constant, ϵ_∞ and the dielectric relaxation time, τ .

$$Q = \frac{(ze)^2(\epsilon_0 - \epsilon_\infty)\tau}{\epsilon_0(2\epsilon_0 + 1)\eta_0} \quad (10)$$

Fernández Prini and Atkinson⁽³⁹⁾ found that for tetraalkylammonium ions in dipolar aprotic solvents, Zwanzig's theory describes quite well the experimental results for the slip condition, but they show systematic deviations in protic solvents (water and alcohols). We confirmed that conclusion for the Bu_4N^+ ion with the aprotic solvents of Table I, for which dielectric parameters are reported.⁽⁴⁰⁾ By plotting $(z^2 e F / \lambda^0 / \eta_0)$ vs. Q for slip conditions, we obtain from Eq. (9) the radius 0.559 nm from the intercept and 0.544 nm from the slope. However, for protic solvents having large Q values, the dielectric friction is largely overestimated by theory.

Gill⁽⁴¹⁾ proposed the following empirical equation to describe the Walden product of ions in pure and mixed nonaqueous solvents, considering perfect slipping:

$$\lambda^0 \eta_0 = \frac{z^2 e F}{6\pi(r - 0.0103\epsilon_0 - r_y)} \quad (11)$$

where r_y is a correction factor, which is 0.085 nm for dipolar nonassociated solvents and 0.113 nm for hydrogen-bonded and other nonassociated solvents. This equation overestimates the Walden product for solvents of high dielectric constant. For instance, it predicts a value of 27.2 S-cm²-mol⁻¹-mPa-s in formamide in complete disagreement with the values reported in Table I.

Hubbard and Onsager^(42,43) developed the most complete continuum theory of ionic friction by solving the Navier–Stokes hydrodynamic equations. In this model, the dielectric friction does not become infinite when the ionic radius tends to zero, but it reaches a constant value, which depends on the viscosity and dielectric parameters of the solvent. The simplest version of the HO theory was formulated by Wolynes⁽⁴⁴⁾ starting with the following expression for the total friction ($\zeta = z^2 e F / \lambda$) of a moving ion in a continuum fluid having a distance-dependent

viscosity:

$$\frac{1}{\zeta} = \int_R^\infty \frac{dr}{4\pi r^2 \eta(r)} \quad (12)$$

where the viscosity is given by:

$$\eta(r) = \eta_0 \left(1 + \frac{R_{\text{HO}}^4}{r^4} \right) \quad (13)$$

R_{HO} being the Hubbard–Onsager radius defined as:

$$R_{\text{HO}} = \frac{\tau e^2 (\epsilon_0 - \epsilon_\infty)}{16\pi \eta_0 \epsilon_0 r^4} \quad (14)$$

Using the dielectric parameters reported for 15 of the solvents⁽⁴⁰⁾ listed in Table I, we calculate R_{HO} for the Bu_4N^+ ion using the crystallographic radius (0.494 nm) and an effective radius of 0.550 nm. The results, shown in Fig. 3, indicate that the HO theory describes quite well the Walden product of the Bu_4N^+ ion when the effective radius is used. The overall picture emerging from this behavior is that the mobility of the Bu_4N^+ ion is not influenced by the dielectric friction and the difference between the effective radius and the crystallographic value could be ascribed to the slip factor used in Eq. (12). Balbuena *et al.*⁽⁴⁵⁾ argued that this factor is not an immediate reflection of the surface boundary conditions and could have a value between 4 and 6.

The Walden product $\lambda^0 \eta$ for the PF_6^- ion increases with the solvent permittivity, as observed in Table II. This result is not surprising since the radius of this ion, 0.295 nm,⁽⁴⁶⁾ is smaller than the Bu_4N^+ ion, and the dielectric friction has to be added to the viscous friction in order to explain the behavior of $\lambda^0 \eta$. However, the HO theory fails to explain the strong decrease of the Walden product with the increase of R_{HO} , as can be seen in Fig. 3. All the data reported in Table II were plotted, except for that for sulfolane due to the lack of information on the dielectric relaxation time of this solvent.

Bagchi and Biswas⁽⁴⁷⁾ have recently shown how a microscopic approach to the friction problem could explain the deviations of the ionic mobilities to the Walden product. In this molecular model, the fast solvation dynamics is found to control the slow mobility of ions in the solvent and the solvent–berg model⁽⁴⁸⁾ can be recovered for small ions in slow solvents. Unfortunately, the calculation of the friction using the molecular model is complex, requires detailed information on the solvent dynamic and the dynamic structure factor of the ion, and is beyond the scope of this work.

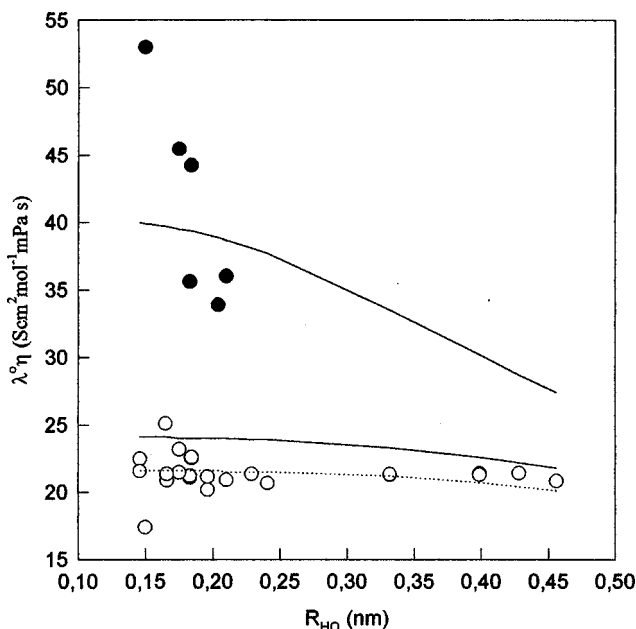


Fig. 3. Walden product for and Bu_4N^+ (○) and PF_6^- (●) in different solvents as a function of R_{HO} . The full lines correspond to the predictions of the HO theory using the crystallographic radii. The dotted lines correspond to the HO theory with $r = 0.55$ nm.

3.4. Electrical Conductivity and Association Constant of $Fe(Cp^*)_2PF_6$ in Organic Solvents

No information is available for the electrical conductance of $Fe(Cp^*)_2PF_6$ or any other salt containing the $Fe(Cp^*)_2^+$ cation. Considering the absence of data, the conductivity of $Fe(Cp^*)_2PF_6$ was measured in four organic solvents of dielectric constant ranging from 35.9 to 8.93.

Conductivity measurements in those solvents with higher dielectric constant (acetonitrile and acetone) were carried out using CELL1, while CELL2 was reserved for those solvents where considerable ionic association was expected (1,2-dichloroethane and dichloromethane). Experiments were also performed at 50°C in 1,2-dichloroethane in order to test the sensitivity of the Walden product to temperature changes. The measured molar conductivities are reported in Table IV.

Molar conductivity data for $Fe(Cp^*)_2PF_6$ in acetonitrile, acetone, 1,2-dichloroethane, and dichloromethane at 25°C were analyzed with Eq. (2), while data in 1,2-dichloroethane at 50°C were treated with Eq. (5) because the precision of the data were not high enough and nonconvergent results were obtained with Eq. (2).

Table IV. Molar Conductivities of $\text{Fe}(\text{Cp}^*)_2\text{PF}_6$ in Organic Solvents

$10^3 C$ (mol-dm ⁻³)	Λ (S-cm ² -mol ⁻¹)	$10^3 C$ (mol-dm ⁻³)	Λ (S-cm ² -mol ⁻¹)
A. Acetonitrile (25°C)		B. Acetone (25°C)	
0.06438	165.48	0.04374	176.68
0.15658	164.60	0.08134	175.40
0.20437	164.23	0.12328	174.11
0.27307	163.49	0.16936	172.50
0.32443	163.26	0.23153	171.55
0.37652	162.82	0.32123	169.62
		0.45976	167.32
C. 1,2-Dichloroethane (25°C)		D. 1,2-Dichloroethane (50°C)	
0.01056	66.52	0.008313	91.81
0.05213	61.60	0.056510	82.54
0.10910	57.89	0.123299	74.58
0.17769	54.62	0.203604	71.90
0.22650	52.46	0.364619	65.97
0.29419	50.60		
0.42300	47.43		
0.48921	46.04		
E. Dichloromethane (25°C)			
0.01713	114.45		
0.02228	111.43		
0.05818	102.01		
0.11550	93.83		
0.18561	86.70		
0.26621	80.50		
0.33518	77.04		

Figure 4 show the deviations of experimental data to the calculated best fit and, in Table V, we compiled the information obtained for $\text{Fe}(\text{Cp}^*)_2\text{PF}_6$ at 25°C.

The molar conductivity of $\text{Fe}(\text{Cp}^*)_2\text{PF}_6$ in acetonitrile indicates that ion association is negligible in this solvent, as recently found for ferrocenium hexafluorophosphate.⁽⁴⁹⁾

The product $\lambda^0\eta$ for $\text{Fe}(\text{Cp}^*)_2\text{PF}_6$ shows a slight dependence on the solvent permittivity, mainly due to the contribution of the PF_6^- anion. Because of its large size, the behavior of the $\text{Fe}(\text{Cp}^*)_2^+$ ion is expected to be similar to that of the Bu_4N^+ ion.

The association constant of $\text{Fe}(\text{Cp}^*)_2\text{PF}_6$ and Bu_4NPF_6 in the solvents studied in this work are shown in Fig. 5 as a function of the reduced temperature⁽⁵⁰⁾ defined by:

$$T_r = \frac{2\epsilon k T r}{|z+z-e^2|} \quad (15)$$

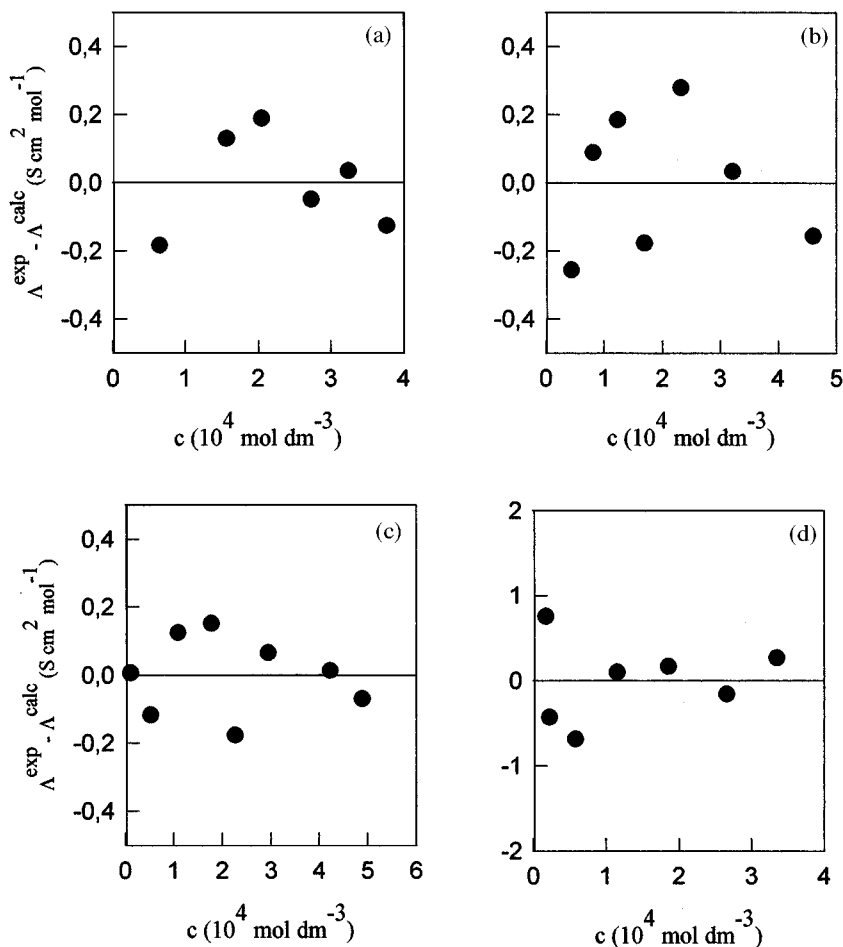


Fig. 4. Conductivity data for $\text{Fe}(\text{Cp}^*)_2\text{PF}_6$ in different solvents at 25°C expressed as deviations from Eq. (2) with the parameters reported in Table V. a) Acetonitrile; b) acetone; c) 1,2 dichloroethane; d) dichloromethane.

The reduced temperature is the parameter that determines the degree of ion-pair formation in the primitive model of electrolytes: the lower T_r , the higher the association constant of the system⁽⁵¹⁾. In the calculation of T_r , we used $r = 0.33 \text{ nm}$ for the $\text{Fe}(\text{Cp}^*)_2^+$ ion, based on bond distances and geometric considerations.

The ion-pair formation in Bu_4NPF_6 is higher than in $\text{Fe}(\text{Cp}^*)_2\text{PF}_6$ despite the larger size of the Bu_4N^+ ion. This could be related to the formation of a solvent separated ion pair in the case of $\text{Fe}(\text{Cp}^*)_2\text{PF}_6$.

Table V. Limiting Molar Conductivities, Association Constants, and Walden Products for $\text{Fe}(\text{Cp}^*)_2\text{PF}_6$ at 25°C

Solvent	Λ^0 ($\text{S}\cdot\text{cm}^2\cdot\text{mol}^{-1}$)	K_A ($\text{dm}^3\cdot\text{mol}^{-1}$)	d_{Bj} (nm)	$\Lambda^0\eta$
Acetonitrile	168.2 ± 0.3	—	0.764	58.2
Acetone	181.4 ± 0.3	$(2.6 \pm 0.5) 10^1$	1.354	55.4
1,2-Dichloroethane	69.3 ± 0.2	$(1.9 \pm 0.3) 10^3$	2.705	54.0
1,2-Dichloroethane ^a	93.8 ± 1.0	$(2.0 \pm 0.6) 10^3$	2.835	54.0
Dichloromethane	123.8 ± 0.8	$(3.8 \pm 0.3) 10^3$	3.138	50.8

^aAt 50°C.

4. CONCLUSIONS

The electrical conductance of Bu_4NPF_6 in acetone was measured at 25°C. From the experimental data, we calculated the infinite dilution electrical conductivity of the salt and its association constant. The ionic conductivities of the Bu_4N^+ and PF_6^- ions at infinite dilution were analyzed in terms of the continuum theories of viscous and dielectric friction. It was concluded that the HO continuum friction model described quite well the behavior of the large Bu_4N^+ ion by using an effective radius, but it fails to explain the conductivity of the PF_6^- ion.

The electrical conductance of $\text{Fe}(\text{Cp}^*)_2\text{PF}_6$ was measured in four organic solvents over a wide range of dielectric permittivities. The observed changes in the Walden product with the permittivity of the solvent was ascribed to the small PF_6^- ion. The association constants of the $\text{Fe}(\text{Cp}^*)_2\text{PF}_6$ in the solvents studied

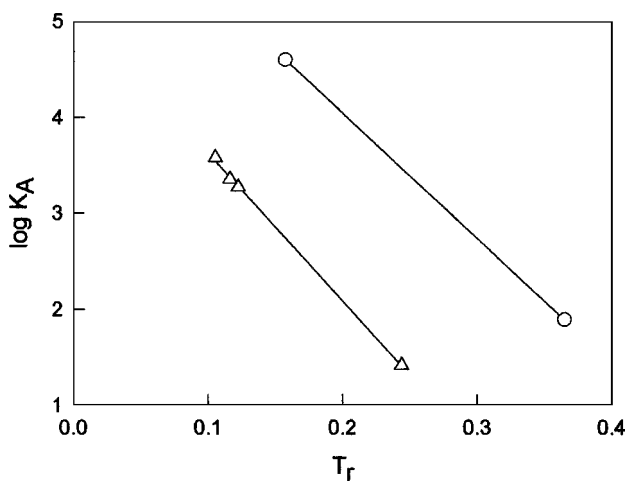


Fig. 5. Association constant of $\text{Fe}(\text{Cp}^*)_2\text{PF}_6$ (Δ) and Bu_4NPF_6 (\circ) as a function of the reduced temperature.

vary with the reduced temperature as expected for the continuum theories, while the lower association, as compared to the BuN_4PF_6 was ascribed to the formation of solvent-separated ion pairs.

ACKNOWLEDGMENTS

H.R.C is a member of Carrera del Investigador Científico del CONICET. Financial support from CONICET is greatly appreciated. D.L.G. thanks CNEA for a graduate fellowship.

REFERENCES

1. J. B. Cooper, A. M. Bond, and K. B. Oldham, *J. Electroanal. Chem.* **331**, 877 (1992).
2. K. B. Oldham, T. J. Cardwell, J. H. Santos, and A. M. Bond, *J. Electroanal. Chem.* **430**, 39 (1997).
3. A. M. Bond, *Analyst* **119**, R1 (1994).
4. S. C. Olsen and D. E. Tallman, *Anal. Chem.* **68**, 2054 (1996).
5. D. L. Goldfarb and H. R. Corti, *Electrochem. Comm.* **2**, 663 (2000).
6. M. Spiro, in *Physical Chemistry of Organic Solvents Systems*, Part 3, Chap. 5, A. K. Covington and T. Dickinson, eds., (Plenum Press, New York 1973).
7. B. S. Krumgalz, *J. Chem. Soc. Faraday Trans. I*, **79**, 571 (1983).
8. T. M. Stockinger, R. J. Lemire, and P. G. Sears, *J. Solution Chem.* **12**, 599 (1983).
9. R. A. Robinson and R. H. Stokes, *Electrolyte Solutions* (Butterworth, London, 1962).
10. M. L. Jansen and H. L. Yeager, *J. Phys. Chem.* **77**, 3089 (1973).
11. R. Zana, J. E. Desnoyers, G. Parron, R. L. Kay, and K. Lee, *J. Phys. Chem.* **86**, 3996 (1982).
12. J. F. Casteel, R. J. Lemire, and P. G. Sears, *J. Solution Chem.* **11**, 55 (1982).
13. J. F. Coetzee and G. P. Cunningham, *J. Amer. Chem. Soc.* **87**, 2529 (1965).
14. P. Bruno, M. P. Della Monica, and E. Righetti, *J. Phys. Chem.* **77**, 1258 (1973).
15. C. J. James and R. M. Fuoss, *J. Solution Chem.* **4**, 91 (1975).
16. B. B. Reynolds and C. A. Kraus, *J. Amer. Chem. Soc.* **70**, 1709 (1948).
17. M. A. Matesich, J. A. Nadas, and D. F. Evans, *J. Phys. Chem.* **74**, 4568 (1970).
18. L. Reichstädter, E. Fischerova, and O. Fischer, *J. Solution Chem.* **22**, 809 (1993).
19. D. S. Gill, *J. Solution Chem.* **8**, 691 (1979).
20. E. Plichta, M. Salomin, S. Slane, and Y. Uchiyama, *J. Solution Chem.* **16**, 225 (1987).
21. R. A. Robinson, J. M. Stokes, and R. H. Stokes, *J. Phys. Chem.* **65**, 542 (1961).
22. P. M. McDonagh and J. F. Reardon, *J. Solution Chem.* **25**, 607 (1996).
23. A. M. Christie and C. A. Vincent, *J. Phys. Chem.* **100**, 4618 (1996).
24. P. M. McDonagh and J. F. Reardon, *J. Solution Chem.* **27**, 675 (1998).
25. R. Fernández Prini and J. E. Prue, *Trans. Faraday Soc.* **62**, 1257 (1966).
26. L. Song and W. C. Troglor, *J. Amer. Chem. Soc.* **114**, 3355 (1992).
27. R. Fernández Prini, in *Physical Chemistry of Organic Solvents Systems*, Part 1, Chapt. 5, A. K. Covington and T. Dickinson, eds., (Plenum Press, New York, 1973).
28. D. M. Duggan and D. N. Hendrickson, *Inorg. Chem.* **14**, 955 (1975).
29. H. Bianchi, H. R. Corti, and R. Fernández Prini, *J. Chem. Soc. Faraday Trans. I*, **83**, 3027 (1987).
30. J. Barthel, F. Feuerlein, R. Neueder, and R. Wachter, *J. Solution Chem.* **9**, 209 (1980).
31. B. A. Younglove and G. C. Straty, *Rev. Sci. Instr.* **41**, 1087 (1970).
32. D. P. Fernández, A. R. H. Goodwin, and J. M. H. Levelt Sengers, *Intern. J. Thermophys.* **16**, 929 (1995).

33. R. M. Fuoss and K. L. Hsia, *Proc. Natl. Acad. Sci. USA* **8**, 1550 (1967).
34. R. Fernández Prini, *Trans. Faraday Soc.* **65**, 3311 (1969).
35. J. C. Justice, In *Comprehensive Treatise of Electrochemistry*, Vol. 5, B. E. Conway, ed., (Plenum Press, New York, 1983), pp. 223.
36. R. M. Fuoss and C. A. Kraus, *J. Amer. Chem. Soc.* **55**, 476 (1933).
37. J. Barthel, G. Schmeer, H. J. Gores, and F. Feuerhein, *Topics in Current Chemistry*. Vol. III (Springer, Heidelberg, 1983).
38. R. Zwanzig, *J. Chem. Phys.* **52**, 3625 (1970).
39. R. Fernández Prini and G. Atkinson, *J. Phys. Chem.* **75**, 239 (1971).
40. M. L. Horng, J. A. Gardecki, A. Papazyan, and M. Maroncelli, *J. Phys. Chem.* **99**, 17311 (1995).
41. D. S. Gill, *J. Chem. Soc. Faraday Trans. I.* **77**, 751 (1981).
42. J. Hubbard and L. J. Onsager, *J. Chem. Phys.* **67**, 4850 (1977).
43. J. Hubbard, *J. Chem. Phys.* **68**, 1649 (1978).
44. P. G. Wolynes, *Annu. Rev. Phys. Chem.* **31**, 345 (1980).
45. P. B. Balbuena, K. P. Johnston, P. J. Rossky, and J.-K. Hyun, *J. Phys. Chem.* **B102**, 3807 (1998).
46. J. F. Reardon, *Electrochim. Acta* **32**, 1595 (1987).
47. B. Bagchi and R. Biswas, *Acc. Chem. Res.* **31**, 181 (1998).
48. H. S. Frank and W. Y. Wen, *Discuss. Faraday Soc.* **24**, 133 (1957).
49. M. W. Lehmann and D. H. Evans, *J. Phys. Chem.* **B102**, 9928 (1998).
50. H. L. Friedman and B. Larsen, *J. Chem. Phys.* **70**, 92 (1979).
51. R. Fernández Prini, H. R. Corti, and M. L. Japas, *High-Temperature Aqueous Solutions: Thermodynamic Properties*, Chap. 3 (CRC Press, Boca Raton, H, 1992.)